

# Two-Stage Image Deblurring with L0 Gradient Minimization and Non-local Refinement<sup>1</sup>

Kai Wang, Liang Xiao, and Zhihui Wei

*Department of Computer Science and Engineering, Nanjing University of Science and Technology, 210094, Nanjing, China*  
*e-mail: wklslx1988@gmail.com*

**Abstract**—An efficient two-stage non-blind deblurring framework is proposed for recovering blurred images progressively. To this date, most approaches commonly solve a single variational regularization problem incorporated with chosen priors, limiting the attained restoration quality. To address this, two different priors are adopted in separated stages to restore an image in a coarse-to-fine manner and each stage follows a variational regularization scheme. In the first stage, salient edges and large scale textures are produced by minimizing the  $\ell_0$  norm of gradient. The intermediate result is then refined by non-local auto regression model in the next stage. Finally, experimental results demonstrate that the proposed methodology is efficient and achieves nice performance.

*Keywords:* image deblurring, variational regularization,  $\ell_0$  gradient minimization, auto regression (AR) model.

**DOI:** 10.1134/S1054661815040082

## INTRODUCTION

Image blur will be inevitably introduced in the image acquisition process which is accompanied by camera shake, object moving, etc. As a primary low-level image processing procedure, numerous deblurring schemes have been proposed, both on blind deblurring [1, 2] and non-blind deblurring. More recently, blind deblurring has captured a majority of attentions. In contrast, relatively less work has focused on non-blind deblurring, that is, restoring the image given known or estimated image blur. Yet, to this date, most blind deblurring [3] approaches are composed of blur estimation and non-blind deblurring, particularly, being an essential sub-problem of blind deblurring. To cope with the ill-posed nature of non-blind deblurring, the regularization-based or Bayesian-based techniques have been widely proposed by regularizing the solution spaces. These techniques are supported on some form of an appropriate prior knowledge about the original image to be estimated and various image models have been developed [4–6]. Since different priors behave in distinct manners, these deblurring approaches commonly share a uniform variational regularization scheme, which barely leads to ideal results due to the limitation of integrated priors.

In this paper, we consider the non-blind deblurring problems from another perspective. Thus we develop an efficient two-stage non-blind deblurring scheme,

aiming to restore an image from coarse to fine. In the first stage, a piece-wise smoothing  $\ell_0$  norm of gradient is adopted to produce an intermediate result which contains sharp edges and part of details. Then in order to refine the coarse estimated result, we introduce non-local constraints to obtain an ideal restored image in the second stage.

## PROBLEM FORMULATION

Let  $\mathbf{y} = (y_1, \dots, y_N)^T$  be the captured image vector. Generally in non-blind deblurring, as the point-spread-function (PSF) is given or estimated, the blur process can be expressed in a matrix-vector form:

$$\mathbf{y} = \mathbf{K}\mathbf{x} + \mathbf{n}, \quad (1)$$

where  $\mathbf{K}$  is a circular convolution matrix of PSF,  $\mathbf{x} = (x_1, \dots, x_N)^T$  is the sharp image vector, and  $\mathbf{n} = (n_1, \dots, n_N)^T$  is the additive Gaussian noise vector.

As being mentioned above, the problem of inferring  $\mathbf{x}$  from the degradation model (1) is usually ill-posed, which means a solution is highly sensitive to a small perturbation of the input. To obtain meaningful estimated images, an efficient strategy is enforcing some form of regularization to penalize undesirable solutions. Accordingly, the variational regularization deblurring problem is formulated as the following unconstrained optimization problem:

$$\hat{\mathbf{x}} = \arg \min_{\mathbf{x}} \left\{ \frac{1}{2} \|\mathbf{y} - \mathbf{K}\mathbf{x}\|_2^2 + \gamma R(\mathbf{x}) \right\}. \quad (2)$$

<sup>1</sup> The article is published in the original.

Here in our two-stage non-blind deblurring method,  $R(\mathbf{x})$  respectively denotes two different regularizer in two stages, and the parameter  $\gamma$  controls the weight we assign to the regularizer.

PROPOSED METHOD

Rather than restoring the whole image from a degraded observation, we suggest that non-blind deblurring can be separated into two stages. Firstly, the salient edges and some large scale details will be recovered. Then more details will be added to produce an ideal result in the next stage consequently. Being similar to paintings, one would establish skeletons of a picture and then increase details in a coarse-to-fine mechanism. The proposed two-stage non-blind deblurring method is introduced as follows.

First Stage

To achieve the goal of restoring the most prominent set of edges, a sparse gradient counting scheme [7] extended to non-blind deblurring is adopted. This prior describes the discrete number of intensity changes among neighboring pixels, and it would yield a piece-wise smoothing solution in an optimization framework. Originally, the gradient measure is expressed as

$$C(\mathbf{x}) = \# \left\{ \sum_{*} |\partial_{*} x_i| \neq 0 \right\}, \tag{3}$$

where  $* \in \{h, v\}$  denotes the horizontal and vertical directions. This measure counts  $i$  whose magnitude  $\sum_{*} |\partial_{*} x_i|$  is not zero.

By integrating it into non-blind deblurring framework,  $\mathbf{x}$  is estimated by solving

$$\min_{\mathbf{x}} \left\{ \|\mathbf{y} - \mathbf{K}\mathbf{x}\|_2^2 + \lambda C(\mathbf{x}) \right\}, \tag{4}$$

where  $\lambda$  is the weight directly controls the significance of  $C(\mathbf{x})$ . Obviously, a large  $\lambda$  makes the result have few edges.

As Eq. (4) involves a discrete counting metric, we also employ a half-quadratic splitting strategy by introducing auxiliary variables to solve the problem above. Denoting the two auxiliary variables  $h_i$  and  $v_i$  corresponding to  $\partial_h x_i$  and  $\partial_v x_i$ , respectively, and reformulating the objective function as

$$\min_{\mathbf{x}, \mathbf{h}, \mathbf{v}} \left\{ \|\mathbf{y} - \mathbf{K}\mathbf{x}\|_2^2 + \lambda C(\mathbf{h}, \mathbf{v}) + \beta \sum_i \left( (\partial_h x_i - h_i)^2 + (\partial_v x_i - v_i)^2 \right) \right\}, \tag{5}$$

where  $C(\mathbf{h}, \mathbf{v}) = \# \{i | |h_i| + |v_i| \neq 0\}$  returns the number of non-zero elements in  $|h| + |v|$ , and  $\beta$  is a weight that we will vary during the optimization. Minimizing Eq. (5) can be performed by two steps, alternatively solving for  $(\mathbf{h}, \mathbf{v})$  and  $\mathbf{x}$ .

Given a fixed  $\mathbf{x}$  from the previous iteration, the  $(\mathbf{h}, \mathbf{v})$  estimation sub-problem corresponds to minimizing

$$\min_{\mathbf{h}, \mathbf{v}} \left\{ \sum_i \left( (\partial_h x_i - h_i)^2 + (\partial_v x_i - v_i)^2 \right) + \frac{\lambda}{\beta} C(\mathbf{h}, \mathbf{v}) \right\}. \tag{6}$$

After some algebraic derivations, the solution for  $(\mathbf{h}, \mathbf{v})$  is

$$(h_i, v_i) = \begin{cases} (0, 0), & (\partial_h x_i)^2 + (\partial_v x_i)^2 \leq \frac{\lambda}{\beta}, \\ (\partial_h x_i, \partial_v x_i), & \text{otherwise,} \end{cases} \tag{7}$$

which has the same form with that in [7].

Given a fixed pair  $(\mathbf{h}, \mathbf{v})$  yielding Eq. (5) to be quadratic in  $\mathbf{x}$ , then the objective function for  $\mathbf{x}$  is

$$\min_{\mathbf{x}} \left\{ \|\mathbf{y} - \mathbf{K}\mathbf{x}\|_2^2 + \beta \left( \|\partial_h \mathbf{x} - \mathbf{h}\|_2^2 + \|\partial_v \mathbf{x} - \mathbf{v}\|_2^2 \right) \right\}. \tag{8}$$

Then we apply Fast Fourier Transform (FFT) which diagonalized the convolution matrix for fast computation. This yields solution directly:

$$\mathbf{x} = F^{-1} \left( \frac{\overline{F(\mathbf{k})} F(\mathbf{y}) + \beta \sum_{*} \overline{F(\partial_{*})} F(\mathbf{z})}{F(\mathbf{k}) F(\mathbf{k}) + \beta \sum_{*} \overline{F(\partial_{*})} F(\partial_{*})} \right), \tag{9}$$

where  $\mathbf{z} \in (\mathbf{h}, \mathbf{v})$  denotes the auxiliary variables.  $F(\cdot)$  and  $F^{-1}(\cdot)$  respectively denote the FFT and inverse FFT, and  $\overline{F(\cdot)}$  is the complex conjugate of  $F(\cdot)$ . The plus, multiplication and division are all component-wise operators.

In this stage, applying the  $\ell_0$  gradient minimization scheme aims to enforce preserving significant edges by confining the number of non-zero gradients, while few details remain. These lead to a coarse estimation  $\mathbf{x}_0$ .

Second Stage

The coarsely estimated image  $\mathbf{x}_0$  is used to establish the relationship between a local patch and its similar “neighbors.” Inspired by non-local based techniques [8], we simply introduce the non-local auto-regression model as a regularizer into the non-blind deblurring framework. To preserve the well restored edges, we enforce the final deblurred result to be close to  $\mathbf{x}_0$  on the edges. Hence we compute the mask  $\mathbf{M}$  (see Fig. 1e) on  $\mathbf{x}_0$  that encodes the edges where the standard derivation of pixel values is larger than a

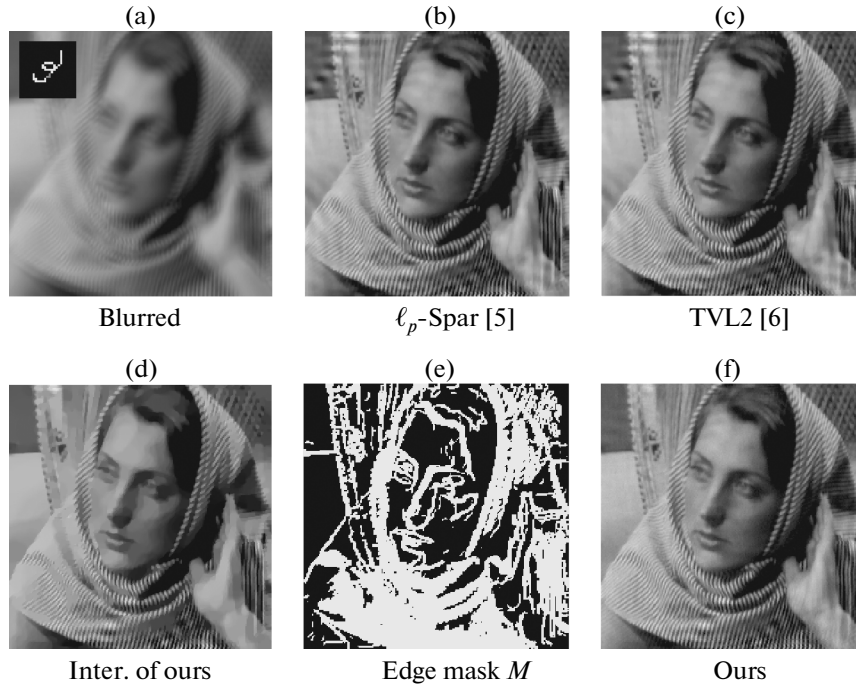


**Fig. 1.** Deblurring performance comparison on image “Barbara.” (a)–(c) Blurred image with an  $27 \times 27$  PSF;  $\ell_p$ -Spar method [5] (PSNR = 27.651, SSIM = 0.891); TVL2 [6] (PSNR = 27.496, SSIM = 0.892); (d)–(f) intermediate result produced by the first stage (PSNR = 26.938, SSIM = 0.840); edge mask  $\mathbf{M}$ ; final result of our method (PSNR = **28.985**, SSIM = **0.918**).

threshold, which is set to 0.06 in the paper. Then the optimization problem can be formulated as,

$$\min_x \left\{ \frac{1}{2} \|\mathbf{y} - \mathbf{K}\mathbf{x}\|_2^2 + \eta \sum_i \left| x_i - \sum_{j \in S_i} \hat{b}_{ij} x_j \right|^2 + \alpha \|\mathbf{M}(\mathbf{x} - \mathbf{x}_0)\|_2^2 \right\}. \tag{10}$$

Here  $\eta$  is the parameter of the non-local regularizer,  $S_i$  is the search region, and  $\hat{b}_{ij}$  is the non-local auto-regression weight can be computed on  $\mathbf{x}_0$  by matching current patch centered at pixel  $x_i$  with other similar patches in region  $S_i$ . The non-local auto regression model indicates that each  $x_i$  can be linear represented by its non-local similar points  $x_j$  ( $j = 1, \dots, L$ ). And  $\alpha$  is the weight of the edge-preserving constraint.

For intuitive computation, we rewritten Eq. (10) into the following equivalent matrix-vector form

$$\min_x \left\{ \frac{1}{2} \|\mathbf{y} - \mathbf{K}\mathbf{x}\|_2^2 + \eta \|(\mathbf{I} - \mathbf{B})\mathbf{x}\|_2^2 + \alpha \|\mathbf{M}(\mathbf{x} - \mathbf{x}_0)\|_2^2 \right\}. \tag{11}$$

Here, the non-local auto regression matrix  $\mathbf{B}$  is the matrix form of  $\hat{b}_{ij}$ . Since this objective function is quadratic in  $\mathbf{x}$ , the global minimum can be easily achieved by gradient descent. The coarse estimation  $\mathbf{x}_0$  is also regarded as an initial input of this stage.

Hence, the proposed two-stage non-blind deblurring framework restores an image in a progressive manner, which can obtain nice results even by employing simple priors.

### RESULTS

To demonstrate the superior performances of the proposed approach, we compare it with two state of the art non-blind deblurring methods, including the hyper-Laplacian prior based method (denoted by  $\ell_p$ -Spar) [5] and the efficient TVL2 algorithm [6]. Experiments are tested on simulated blurred images. The basic parameter setting of the proposed method is as follows: the comparison patch size in computing non-local weights is  $5 \times 5$ , the search window is with size  $25 \times 25$ , and empirically, the three regularization parameters  $\lambda$ ,  $\alpha$ , and  $\eta$  are respectively set as  $5e-5$ , 0.01, and 0.05.

The visual comparison of the non-blind deblurring methods are shown in Fig. 1, from which we can see that our two-stage method produces much cleaner results. Obviously, our results contain more details than other methods. The proposed method achieves an intermediate result with few details in the first stage, however, more details are recovered that benefits from applying non-local constraints. Since in the first stage, the smoothing regularizer can suppress ringing artifacts and some other outliers,

PSNR/SSIM results of different deblurring methods

Image	Kernel	$\ell_p$ -Spar [5]	TVL2 [6]	Inter. of ours	Ours
Parrot	1	37.854/0.969	37.207/0.958	35.188/0.924	<b>40.278/0.972</b>
	2	36.087/0.955	35.152/0.937	34.275/0.916	<b>38.974/0.965</b>
	3	38.147/ <b>0.973</b>	38.243/0.969	35.299/0.936	<b>38.900/0.971</b>
	4	33.666/0.942	34.019/0.941	35.524/0.911	<b>34.859/0.953</b>
Starfish	1	32.398/0.966	31.175/0.941	31.389/0.932	<b>35.343/0.974</b>
	2	30.177/0.931	28.601/0.899	30.409/0.913	<b>34.130/0.962</b>
	3	33.812/0.971	33.375/0.962	32.273/0.943	<b>34.706/0.975</b>
	4	30.159/0.953	30.066/0.948	29.245/0.923	<b>30.682/0.960</b>
Hat	1	35.387/0.961	34.049/0.938	33.821/0.920	<b>38.616/0.965</b>
	2	34.005/0.940	32.810/0.914	33.060/0.903	<b>37.393/0.955</b>
	3	35.953/ <b>0.966</b>	35.647/0.956	33.962/0.925	<b>36.777/0.963</b>
	4	33.166/0.938	33.447/0.937	31.927/0.899	<b>34.110/0.943</b>
Girl	1	34.517/0.925	33.935/0.927	32.302/0.825	<b>38.586/0.962</b>
	2	31.783/0.895	30.863/0.885	30.848/0.801	<b>35.834/0.948</b>
	3	33.480/0.925	33.783/0.946	31.808/0.838	<b>34.747/0.955</b>
	4	31.466/0.871	31.677/0.901	30.509/0.798	<b>33.127/0.922</b>
Boat	1	32.161/0.948	30.583/0.909	31.475/0.916	<b>36.301/0.969</b>
	2	29.213/0.910	27.853/0.871	29.488/0.888	<b>32.590/0.948</b>
	3	32.524/0.956	31.826/0.942	31.539/0.926	<b>33.639/0.965</b>
	4	29.434/0.947	29.127/0.935	28.809/0.915	<b>29.990/0.953</b>
Man	1	33.156/0.952	31.937/0.916	32.275/0.923	<b>35.529/0.960</b>
	2	32.352/0.934	30.917/0.892	31.943/0.910	<b>35.615/0.953</b>
	3	34.033/ <b>0.965</b>	33.857/0.957	32.717/0.931	<b>34.785/0.962</b>
	4	31.588/0.946	31.706/0.946	30.498/0.904	<b>32.200/0.947</b>

our results contain fewer artifacts than the compared methods.

To quantitatively verify our performances, the PSNR and SSIM results on a set of 24 images generated by 6 photographic images and 4 ground-truth motion blur kernels (selected from Levin et al.'s testing dataset [9]) are reported in table, from which we can conclude that the proposed two-stage non-blind deblurring method outperforms the other competing methods [5, 6]. In average, we strongly outperform the efficient half-quadratic regularization approach of Krishnan et al. [5] by 3 dB.

## CONCLUSIONS

We proposed a novel framework for non-blind deblurring which is composed of two separated stages. To achieve these, two efficient priors were respectively adopted in the two stages. The  $\ell_0$  norm of gradient was used for recovering salient edges, then the non-local auto regression model was applied for refinement. Experimental results demonstrated that the proposed two-stage non-blind deblurring method can achieve highly competitive performance to other leading deblurring methods.

## ACKNOWLEDGMENTS

The authors thank to the reviewers for valuable comments that helped improve the clarity of presentation of this paper. This work was supported in part by the National Nature Science Foundation of China under grant nos. 61101198 and 61171165.

## REFERENCES

1. S. Cho and S. Lee, "Fast motion deblurring," *ACM Trans. Graph.* **145** (8), 1–8 (2009).
2. L. Xu and J. Jia, "Two-phase kernel estimation for robust motion deblurring," in *Proc. ECCV 2010* (Heraklion, 2010), pp. 157–170.
3. R. Fergus, B. Singh, A. Hertzmann, S. T. Roweis, and W. T. Freeman, "Removing camera shake from a single photograph," *ACM Trans. Graph.* **25** (3), 787–794 (2006).
4. K. Dabov, A. Foi, V. Katkovnik, and K. Egiazarian, "Image restoration by sparse 3D transform-domain collaborative filtering," *Proc. SPIE* **6812** (07), 1–12 (2008).
5. D. Krishnan and R. Fergus, "Fast image deconvolution using hyper-Laplacian priors," in *Proc. Neural Information Processing Systems Conf.* (Vancouver, 2009), pp. 1033–1041.
6. Y. Wang, J. Yang, W. Yin, and Y. Zhang, "A new alternating minimization algorithm for total variation image reconstruction," *SIAM J. Imaging Sci.* **1** (3), 248–272 (2008).
7. L. Xu, C. Lu, Y. Xu, and J. Jia, "Image smoothing via L0 gradient minimization," *ACM Trans. Graph.* **30** (6) (2011).
8. A. Buades, B. Coll, and J. M. Morel, "A review of image denoising algorithms, with a new one," *Multiscale Model. Simul.* **4** (2), 490–430 (2005).
9. A. Levin, Y. Weiss, F. Duarand, and W. T. Freeman, "Understanding and evaluating blind deconvolution algorithms," in *Proc. CVPR* (Miami, 2009), pp. 1964–1971.



**Kai Wang** received the BSc degree in science of information and computation from Nanjing University of Science and Technology, Nanjing, Jiangsu, China, in 2010. He is currently pursuing his PhD degree in pattern recognition and intelligent system from Nanjing University of Science and Technology. His research interests are in mathematical image processing and the theory of image modeling. His current research is focused on high-quality image deblurring and video deblurring.



**Liang Xiao** received B.Sc., degree in Applied Mathematics and Ph.D. degree in Computer Science from Nanjing University of Science and Technology (NUST), Nanjing, Jiangsu, China, in 1999 and 2004, respectively. From 2006 to 2008, he was a Post-doctor Research Fellow at the Pattern Recognition Laboratory of the NUST. From 2009–2010, he was a post-doctor at Rensselaer Polytechnic Institute (RPI), USA. He is currently an Associate Professor at the School of Computer Science of NUST. His main research areas include inverse problems in image processing, scientific computing, data mining, and pattern recognition.



**Zhihui Wei** received B.Sc., M.Sc., and Ph.D. degrees from South East University, Nanjing, Jiangsu, China, in 1983, 1986, and 2003, respectively. He is currently the professor and doctoral supervisor of Nanjing University of Science and Technology. His main research interests are mathematical image processing, image modeling, multiscale analysis, video and image coding and compressing, watermarking and steganography, and speech and audio processing. His current research is focused on the theory of image sampling, multiscale geometrical analysis, sparse representation, and partial differential equations.